Single-Molecule Spectroscopy and Dynamics at Room Temperature

X. SUNNEY XIE

Environmental Molecular Sciences Laboratory, Pacific Northwest National Laboratory,† P.O. Box 999, Richland, Washington 99352

Received May 31, 1996

Introduction

Chemists are used to visualizing molecular properties and chemical changes on a single-molecule basis. Holding a molecular model, we can predict the forces with surrounding molecules and conceive a chemical reaction. In contrast, information regarding molecular interactions and chemical dynamics has been primarily derived from experiments conducted on large ensembles of molecules. Although ensemble-averaged results are essential, they often preclude detailed information. This is particularly true in condensed media due to (1) heterogeneity of properties for different molecules, and (2) fluctuations of individual molecules and their interacting environments.

The spirit of studying single-molecule behaviors dates back to the turn of the century. In addition to Einstein's well-known work on Brownian motion, there has been a tradition for studying single "macromolecules" or a small number of molecules either by light scattering or by fluorescence using an optical microscope. Modern computers have allowed detailed studies of single-molecule behaviors in condensed media through molecular dynamics simulations.[1] Advances in scanning tunneling microscopy (STM) and atomic force microscopy (AFM) have allowed the visualization and even manipulation of single atoms and molecules.[2,3] Optical spectroscopy offers a wealth of information on the structure, interaction, and dynamics of molecular species. With the motivation of removing "inhomogeneous broadening", spectroscopic techniques have evolved from spectral hole burning, fluorescence line narrowing, and photo-echo to the recent pioneering work on single-molecule spectroscopy in solids at cryogenic temperatures.[4] High-resolution spectroscopic work on single molecules[5] relies on zero phonon lines which appear at cryogenic temperatures, and have narrow line widths and large absorption cross sections.

Recent advances in near-field and confocal fluorescence microscopy have allowed not only fluorescence imaging of single molecules with high spatial resolutions but also conducting single-molecule spectroscopy at room temperature. Needless to say, it is important to be able to work at room temperature where most biochemical reactions take place. These advances offer exciting new possibilities in addressing a wide range of problems in many disciplines, such as analytical chemistry, materials research, and, in particular, biological sciences. In this Account, I will provide a physical chemist's perspective on experimental and theoretical developments on room-temperature single-molecule spectroscopy and dynamics, with the emphasis on the information obtainable from single-molecule experiments. For discussions on technical developments, readers are referred to two recent review articles.[6,7]

Xiaoliang Sunney Xie was born in Beijing, China, in 1962. He received a B.Sc. in chemistry at Peking University in 1984, followed by a Ph.D. in chemistry from the University of California at San Diego in 1990 under the guidance of Professor John Simon. After two years of postdoctoral research with Professor Graham Fleming at the University of Chicago, he joined the newly founded Environmental Molecular Sciences Laboratory at Pacific Northwest National Laboratory, where he is currently a chief scientist. His main research interests are single-molecule spectroscopy, near-field microscopy, condensed phase dynamics, and photosynthesis.

Single-Molecule Spectroscopic Measurements with Near-Field and Far-Field Fluorescence Microscopes

Near-field scanning optical microscopy (NSOM) involves scanning a light source, much smaller than the optical wavelength, near the surface of a sample. The spatial resolution of NSOM is limited by the size of the light source, rather than by the diffraction limit. The diffraction limit arises from the diffraction effect at the far field and limits the resolution of conventional optical microscopes to about half of the wavelength. The developments in NSOM have been extensively reviewed.[8−11] Room-temperature near-field fluorescence imaging of single dye molecules was first demonstrated by Betzig and Chichester.[12]

Figure 1A shows our near-field fluorescence image of single oxazine 720 molecules dispersed on a poly(methyl methacrylate) (PMMA) film. The image was obtained by raster-scanning the sample beneath an illuminating NSOM tip[8] and collecting the emission through a transmissive substrate. Figure 1B shows the approximate dimension of the NSOM tip. The end aperture of the tapered optical fiber is confined by the

† Pacific Northwest National Laboratory is operated for the U.S. Department of Energy by Battelle Memorial Institute.

(1) See, for example, Allen, M. P.; Tildesley, D. J. *Computer Simulation of Liquids*; Oxford University Press: Oxford, 1987.
(2) For a review on chemical applications, see: Avouris, P. *Acc. Chem. Res.* **1995**, *28*, 95.
(3) For a review on biological applications, see: Bustamante, C.; Keller, D. *Phys. Today* **1995**, *48*, 32.
(4) For a recent review, see: Skinner, J. L.; Moerner, W. E. *J. Phys. Chem.* **1996**, *100*, 13251.
(5) Moerner, W. E. *Acc. Chem. Res.* **1996**, *29*, 563 and references therein.
(6) Trautman, J. K.; Macklin, J. J. *Chem Phys.* **1996**, *205*, 221.
(7) Xie, X. S.; Bian, R. X.; Dunn, R. C. In *Focus on Multidimensional Microscopy*; Chen, P. C., Hwang, P. P., Wu, J. L., Wang, G., Kim, H., Eds.; World Scientific: River Edge, NJ, 1997; Vol. 1.
(8) Betzig, E.; Trautman, J. K. *Science* **1992**, *257*, 189.
(9) Pohl, D. W. In *Advances in Optical and Electron Microscopy*; Mulvey, T., Sheppard, C. J. R., Eds.; Academic Press: New York, 1991; Vol. 12, p 243.
(10) Kopelman, R; Tan, W. *Appl. Spectrosc. Rev.* **1994**, *29*, 39.
(11) Paesler, M; Moyer, P. *Near-field Microscopy*; John Wiley & Sons: New York, 1996.
(12) Betzig, E.; Chichester, R. J. *Science* **1993**, *262*, 1422.

S0001-4842(95)00246-9 CCC: $12.00

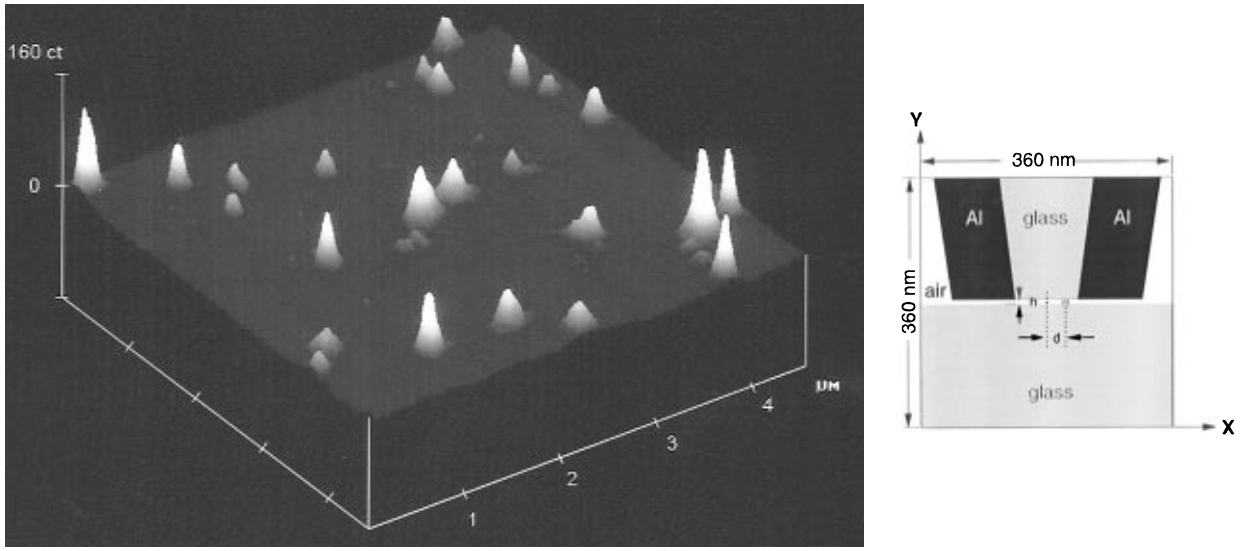

Figure 1. (A, left) Near-field fluorescence image (4.5 μm × 4.5 μm) of single oxazine 720 molecules dispersed on the surface of a PMMA film. Each subdiffraction peak (FWHM 100 nm) is due to a single molecule. The different intensities are due to different molecular orientations and single-molecule spectra. (B, right) Schematic of the NSOM tip with an aperture diameter of 96 nm. This area is divided into a 300 × 300 grid of 1.2 nm square cells for FDTD simulations.

aluminum coating, resulting in a 100-nm resolution (full width at half maximum, FWHM) for the single-molecule image. At the near field of the aperture are strong nonpropagating evanescent field components that decay rapidly with distance from the aperture. Recently, the electromagnetic field around the aluminum-coated NSOM tip has been calculated using the multiple multipole method[13] and the finite difference time domain (FDTD) method,[14,15] both of which numerically solve the Maxwell equations for the specific geometry of the NSOM tip.

To quantitatively predict the signal strength of molecular fluorescence, one cannot simply use the absorption cross section and the photon flux to the far field, but must evaluate the electric dipole matrix element:

$$\langle \psi_i(x,y,z)|\mathbf{E}(x,y,z,t)\cdot e\mathbf{r}|\psi_f(x,y,z)\rangle \qquad (1)$$

Unlike the case in conventional spectroscopy, the electric field, **E**, cannot be extracted from the bracket representing a spatial integration over the molecular coordinates (x,y,z) if **E** varies within the dimension of the ground and excited state wave functions, $\psi_i(x,y,z)$ and $\psi_f(x,y,z)$. It was proposed that the selection rules could be different in this situation.[16] However, if **E** varies in the laboratory coordinates (X,Y,Z) within a dimension much larger than the sizes of the wave functions (1 nm), as is the case in Figure 1B, eq 1 becomes

$$\mathbf{E}(X,Y,Z,t)\cdot\langle \psi_i(x,y,z)|e\mathbf{r}|\psi_f(x,y,z)\rangle \qquad (2)$$

i.e., the transition dipole can be viewed as a point dipole, and the same selection rules as in conventional spectroscopy hold. Equation 2 also provides the basis for determining the molecular orientation of a single molecule in all three dimensions, which was elegantly demonstrated by Betzig and Chichester.[12]

In collecting Figure 1A, excitation light linearly polarized along the X axis was coupled into the NSOM tip (Figure 1B). **E** is parallel to the sample surface (along the X axis) beneath the center of the aperture, but perpendicular to the sample surface (along the Y axis) near the edges of the near-field aperture.[12−14] For a molecule with a transition dipole parallel to the sample surface, the pattern of its near-field fluorescence image should have a high intensity at the center due to the maximum overlap between the dipole and electric field. On the other hand, for a molecule with a transition dipole perpendicular to the sample surface, a pattern of two arcs with zero intensity at the center should be seen.[12] Neither this pattern nor any asymmetric patterns are seen in Figure 1A, and we therefore conclude that the molecular transition dipoles are essentially parallel to the PMMA surface. The orientations within the surface plane can be determined by a 90° rotation of the input polarization. We note that conventional polarization measurements are capable of determining the mean orientation only, but not the distribution of orientations.

Immediately after the demonstration of single-molecule imaging with NSOM, room-temperature single-molecule spectroscopy work emerged. Single-molecule emission spectra,[17] fluorescence lifetimes,[18,19] and excitation spectra[7] in ambient environments have been demonstrated. The initial experiments raised many mystifying questions regarding the interaction of the molecule with the NSOM tip and the nature of room-temperature single-molecule spectroscopy. These questions are essential to extract useful information from single-molecule experiments, and will be addressed below.

Room-temperature single-molecule fluorescence detection in solution[20] and in aerosol particles[21] has been

(13) Novotny, L.; Pohl, D. W. In *Photons and Local Probes*; Marti; O., Moller, R., Eds.; Kluwer Academic Publishers: Dordrecht, The Netherlands, 1995; p 21.
(14) Christensen, D. A. *Ultramicroscopy* **1995**, *57*, 189.
(15) Kann, J. L. Ph.D. Dissertation, University of Arizona, Tucson, 1995.
(16) Grober R. D.; Harris, T. Presentation at the Second International Conference of Near-field Optics, Raleigh, NC, 1993.
(17) Trautman, J. K.; Macklin, J. J.; Brus, L. E.; Betzig, E. *Nature* **1994**, *369*, 40.
(18) Ambrose, W. P.; Goodwin, P. M.; Martin, J. C.; Keller, R. A. *Science* **1994**, *265*, 364.
(19) Xie, X. S.; Dunn, R. C. *Science* **1994**, *265*, 361.
(20) For a review, see Keller, R. A; Ambrose, W. P.; Goodwin, P. M.; Jett, J. H.; Martin, J. C.; Wu, M. *Appl. Spectrosc.* **1996**, *50*, 12A.

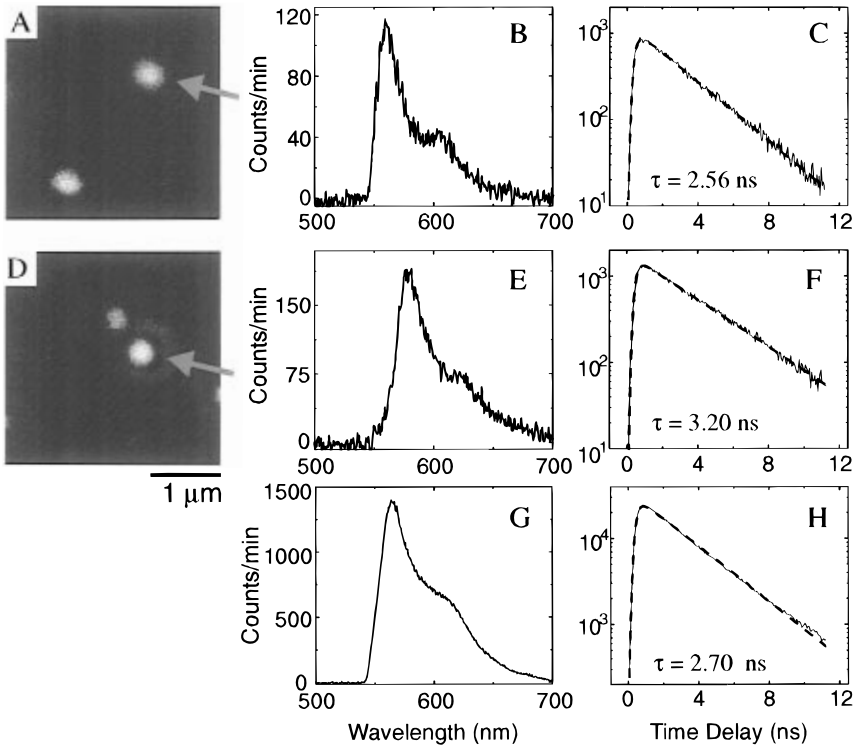

Figure 2. Far-field fluorescence images (A and D), corresponding spectra (B and E), and fluorescence decays (C and F) for two diI molecules located at a PMMA−air interface. The peak emission wavelength was 560 nm in (B) and 578 nm in (E). Lifetimes were fit to a single exponential (dotted curves), with time constants of 2.56 ns ($\chi^2 = 1.05$) in (C) and 3.20 ns ($\chi^2 = 1.16$) in (F). For comparison, the ensemble-averaged spectrum and fluorescence decay are shown in (G) and (H). An exponential fit to the latter yielded a decay time of 2.70 ns ($\chi^2 = 6.7$). This χ^2 is indicative of a large deviation from single-exponential behavior, reflecting the ensemble average over a distribution of lifetimes. Reprinted with permission from ref 25. Copyright 1996 American Association for the Advancement of Science.

demonstrated. In particular, confocal[22,23] and two-photon[24] microscopies have enhanced the sensitivity for solution phase single-molecule detection. Recently, Macklin et al. have obtained a superior sensitivity using far-field optics that allowed collection of room temperature emission spectra and fluorescence lifetimes of single molecules on a surface.[25] Figure 2 shows the far-field images, spectra, and lifetimes of two 1,1′-dioctadecyl-3,3,3′,3′-tetramethylindocarbocyanine (diI) molecules at the surface of a PMMA film. The significant differences in spectra and lifetimes between the molecules reflect the detailed information pertinent to specific local environments, which is not available from the ensemble-averaged spectrum (Figure 2G) and lifetime (Figure 2H).

If no subdiffraction spatial resolution is required and the only goal is to study single-molecule behaviors in a dilute sample, the far-field technique is the judicious choice because of its simplicity, higher sensitivity, and lack of tip perturbations. The advantages of the near-field technique are its higher spatial resolution and ability to correlate spectroscopic information with topographic information.[8] The need to conduct spectroscopic measurements on chemical systems at a nanometric dimension, for example, to study molecular aggregates[26] and to map photosynthetic membranes,[27] etc., has motivated many researchers to use and improve the near-field technique. However, one has to pay a price; the molecule−tip interaction can perturb some spectroscopic measurements. Understanding the interactions between a single molecule and a nanostructure is not only essential for near-field measurements but also relevant to far-field experiments.

Single-Molecule Emission Characteristics near a Nanostructure

In demonstrating single-molecule fluorescence lifetime measurements with NSOM, Ambrose et al.[18] and Xie and Dunn[19] observed the dependency of lifetime on the lateral displacement of the NSOM tip relative to the molecule. As shown in Figure 3A, the fluorescence lifetimes for a sulforhodamine 101 molecule with a horizontal dipole shortened as the molecule approached the tip edges, with the tip−molecule gap held at $h = 7$ nm. This effect was attributed to nonradiative energy transfer to the aluminum coating of the NSOM tip.[18,19] Interestingly, however, Trautman and Macklin later observed the reversed behavior, the lengthening of fluorescence lifetimes near the tip edges,[6] which is associated with a radiative mechanism. This observation was confirmed by us for a larger tip−molecule gap of $h = 20$ nm, as is shown in Figure 3B, and the apparent controversy has recently been resolved.[28]

Molecular fluorescence in front of an interface (dielectric or metallic) was extensively studied in the

(21) Barnes, M. D.; Whitten, W. B.; Ramsey, J. M. *Anal. Chem.* **1995**, *67*, 418 A.
(22) Nie, S.; Chiu, D. T.; Zare, R. N. *Science* **1994**, *266*, 1018.
(23) Eigen, M.; Rigler, R. *Proc. Natl. Acad. Sci. U.S.A.* **1994**, *91*, 5740.
(24) Mertz, J.; Xu, C.; Webb, W. W. *Opt. Lett.* **1995**, *20*, 2532.
(25) Macklin, J. J.; Trautman, J. K.; Harris, T. D.; Brus, L. E. *Science* **1996**, *272*, 255.
(26) Higgins, D. A.; Kerimo, J.; Vanden Bout, D. A.; Barbara, P. F. *J. Am. Chem. Soc.* **1996**, *118*, 4049 and references therein.
(27) Dunn, R. C.; Holtom, G. R.; Mets, L.; Xie, X. S. *J. Phys. Chem.* **1994,** *98*, 3094.
(28) Bian, R. X.; Dunn, R. C.; Xie, X. S.; Leung, P. T. *Phys. Rev. Lett.* **1995**, *75*, 4772.

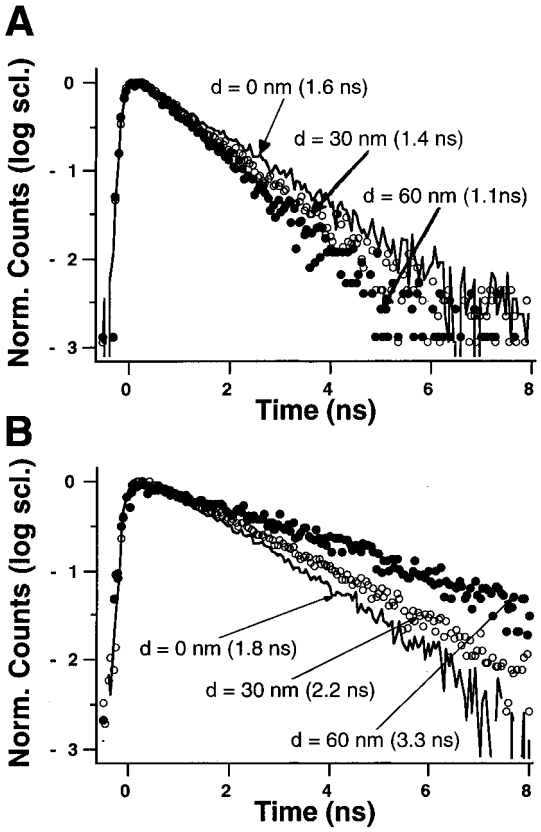

Figure 3. (A) Fluorescence decays of a single sulforhodamine 101 molecule with a horizontal dipole measured at three lateral displacements from the tip center, $d \sim 0$, 30, and 60 nm, with a tip−molecule gap $h \approx 5$ nm. Under this condition, the lifetime is the longest at the tip center and shortened at the tip edge. B) The opposite trend in lifetime is seen at a larger tip−molecule gap of $h \sim 20$ nm. Reprinted with permission from ref 28. Copyright 1995 American Institute of Physics.

1970s and 1980s, and is discussed in several excellent review articles.[29−31] If a fluorescent molecule is located at a distance greater than nanometers away from an interface (of any arbitrary shape), the radiating dipole can be treated classically as a damped-harmonic dipole, $\mu(t)$, driven by its own electric field reflected from the interface:

$$\ddot{\mu} + \omega_o^2 \mu = \frac{e^2}{m} E_R - \gamma_o \dot{\mu} \tag{3}$$

where γ_o and ω_o are the decay rate and emission frequency in the absence of the interface, respectively, and E_R is the reflected electric field projected onto the dipole direction. e and m are the electron charge and mass, respectively. In the presence of the interface, both $\mu(t)$ and $E_R(t)$ oscillate with a slightly shifted frequency ($\omega_o + \Delta\omega$) and decay with a modified rate γ:

$$\mu(t) = \mu_o \cos[(\omega_o + \Delta\omega)t] e^{-\gamma t/2} \tag{4}$$

$$E_R(t) = E_o \cos[(\omega_o + \Delta\omega)t - \phi] e^{-\gamma t/2} \tag{5}$$

Knowing the amplitude E_o and the phase ϕ of $E_R(t)$, we can calculate the modified fluorescence lifetime and frequency shift as follows:[28,30]

$$\frac{\gamma}{\gamma_o} = 1 + \frac{3qn^2}{2\mu_o k^3} E_o \sin\phi \tag{6}$$

$$\frac{\Delta\omega}{\gamma_o} = -\frac{3qn^2}{4\mu_o k^3} E_o \cos\phi \tag{7}$$

where q is the intrinsic fluorescence quantum yield (in the absence of the interface), n is the refractive index of the medium surrounding the molecule, and k is the propagation constant ($k = \omega_o n/c$) in that medium. Using the solution of the reflected field derived by Sommerfeld,[32] Chance, Prock, and Silbey developed a framework for molecular fluorescence in front of an infinite and flat interface.[30] However, for an interface of any arbitrary geometry, such as the one for the NSOM tip shown in Figure 1B, one has to rely on numerical solutions for E_o and ϕ.

Bian et al. have recently carried out a numerical simulation[28] using the FDTD approach.[33] The essence of this approach is to numerically integrate Maxwell's equations for the area in Figure 1B which is divided with a 300 × 300 grid of 1.2 nm square cells, each with the corresponding dielectric constant. For aluminum cells, the frequency dependent dielectric constant is derived from the free electron model. The molecular dipole is simulated as a Hertzian dipole, of which E_o and ϕ are evaluated at the dipole position. Following ref 30, we separated the contributions from radiative (γ_r) and nonradiative ($\gamma_{nr} = \gamma - \gamma_r$) energy transfer rates. γ_r is the decay rate due to radiation going to the far field from the molecular dipole and the induced polarization in the surrounding media. γ_{nr} is the decay rate due to energy dissipation into the absorbing medium (aluminum). By integrating the Poynting vectors around a closed boundary encompassing the molecule and the tip, we calculated γ_r and the apparent emission quantum yield, $q' = \gamma_r/\gamma$, which gives the fraction of energy released by the molecule as radiation going to the far field. Plotted in Figure 4 are the simulated E_o, ϕ, normalized lifetimes τ/τ_o ($=\gamma_o/\gamma$), normalized radiative rates γ_r/γ_o, nonradiative rates γ_{nr}/γ_o, apparent quantum yields q', and spectral shifts $\Delta\omega/\gamma_o$ for both a horizontal and a vertical dipole with intrinsic quantum yields $q = 1$.

The simulated lifetime behavior for a horizontal dipole shown in Figure 4c is consistent with the experimental results in Figure 3. Interestingly, for the small gap, the apparent quantum yield q' (Figure 4f) is significantly reduced at the tip edges due to the increased nonradiative energy transfer rate, γ_{nr} (Figure 4e). On the other hand, for the larger gap, the fluorescence decay is dominated by the radiative rate, γ_r (Figure 4d), which is reduced at the tip edges (opposite of γ_{nr}). As a result, q' remains close to unity across the tip. These results clearly demonstrate that the origin for the reversal in lifetime observed at different tip−molecule gaps results from the competition between the radiative and nonradiative mechanisms.

The FDTD simulation not only yielded physical insight to the experimental observations, but also provided guidance for conducting nonperturbative NSOM experiments.[28] According to Figure 4g,n, the

(29) Drexahage, K. H. In *Progress in Optics XII*; Wolf, E., Ed.; North-Holland: Amsterdam, 1974; p 165.
(30) Chance, R. R.; Prock, A.; Silbey, R. *Adv. Chem. Phys.* **1978**, *37*, 1.
(31) Metiu, H. *Prog. Sur. Sci.* **1984**, *17*, 153.
(32) Sommerfeld, A. *Partial Differential Equations of Physics*; Academic Press: New York, 1949.
(33) Taflove, A. *Computtaional Electrodynamics - the Finite-Difference Time-Domain Method*; Artech House: Boston, 1995.

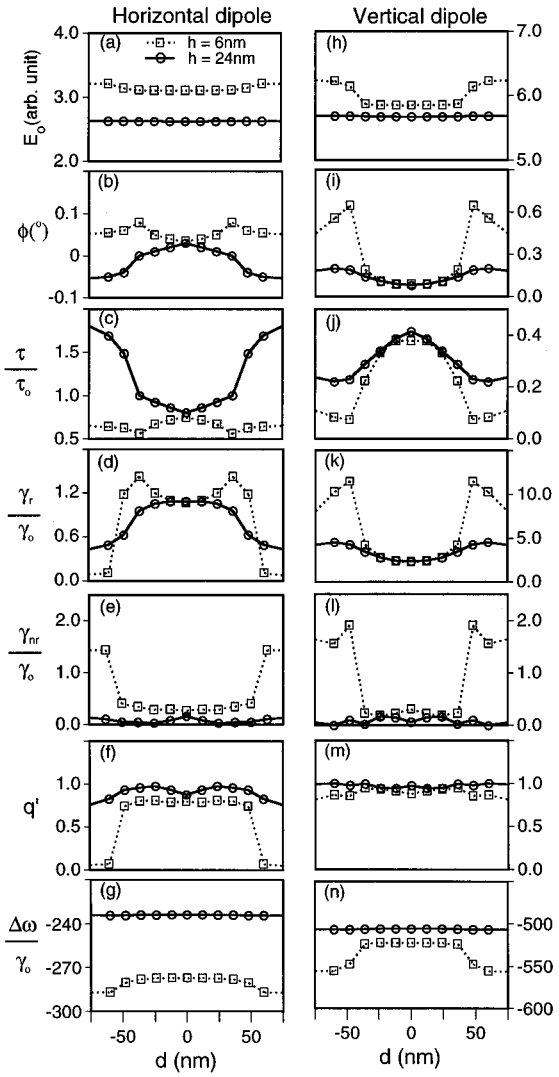

Figure 4. FDTD simulation results for both a horizontal dipole (left column, a−g) and a vertical dipole (right column, h−n) as a function of the lateral displacement, *d*, evaluated at tip−molecule gaps $h = 6$ and 24 nm. From top to bottom, the quantities simulated are the reflected field amplitude E_o and phase ϕ, normalized lifetime τ/τ_o, normalized radiative rate γ_r/γ_o and nonradiative rate γ_{nr}/γ_o, apparent quantum yield q', and spectral shift $\Delta\omega/\gamma_o$. An intrinsic quantum yield $q = 1$ is assumed. Reprinted with permission from ref 28. Copyright 1995 American Institute of Physics.

spectral frequency can be red-shifted by $(1-2) \times 10^{10}$ Hz for a typical dye molecule with $\gamma_o \approx 3 \times 10^8$ s^{-1}. Fortunately, this spectral shift is negligible at room temperature given the broad single-molecule spectral widths (Figure 2). The nonradiative energy transfer can be minimized by centering the tip above the molecule, while changes of the radiative rate can hardly be avoided. Fortunately, for dynamic processes that are much faster than the radiative and nonradiative energy transfer processes, e.g., fast electron transfer reactions, fluorescence lifetimes can be measured with negligible perturbations. This is evident from eq 6; when the intrinsic quantum yield, *q*, is much less than 1, then $\gamma/\gamma_o \approx 1$.

The FDTD approach to spectroscopy represents a new methodology that allows predictions of molecular emission properties in front of an interface of any arbitrary geometry. Recently, other numerical methods for solving Maxwell's equations, such as Green's function approach,[34] a field expansion technique,[35] and the discrete dipole approximation[36] have also been developed. The application of all these approaches will not only provide understanding of near-field spectroscopy, but also shed light on molecular spectroscopy on corrugated surfaces, such as surface-enhanced spectroscopy.[31] Surface-mapping techniques such as STM or AFM can directly provide the surface profile as the input to those simulations, which can in turn be compared with near-field or far-field single-molecule spectroscopic measurements.

Even for far-field experiments on a flat dielectric surface, single-molecule radiative rates have been shown to be dependent on electromagnetic boundary conditions.[25] With the electromagnetic interaction with the surrounding medium understood, one can now concentrate on studying intrinsic behaviors of single molecules.

Probing Single-Molecule Dynamics on the $10^{-2}-10^{3}$-s Time Scale

It is now experimentally feasible to observe single events, such as diffusional motions, spectral shifts, and chemical changes of individual molecules on the $10^{-2}-10^{3}$-s time scale. However, detailed dynamical information requires recording and analyzing single-molecule trajectories, i.e., the temporal evolution of experimental observables. Unlike ensemble-averaged results, each single-molecule trajectory, in principle, cannot be experimentally repeated due to its stochastic nature. Only the statistical properties of the trajectory are repeatable. Although a large number of trajectories of many molecules are needed to reflect the ensemble behavior, single trajectories can often reveal detailed information that is otherwise lost in ensemble-averaged results. A major experimental difficulty in recording long trajectories is photobleaching after 10^5-10^8 excitation cycles. Although the detailed mechanism for photobleaching is as yet unknown, fast bleaching in aerobic environments is primarily due to singlet oxygen.[37]

In demonstrating room-temperature emission spectra of single molecules with near-field microscopy, Trautman et al. observed that the emission spectra of single DiI molecules dispersed on a PMMA film change with time.[17] This room-temperature spectral fluctuation occurs on a peculiarly long time scale. Meanwhile, Ambrose et al.[38] and Xie and Dunn[19] observed sudden intensity jumps in the emission intensity from single rhodamine molecules dispersed on a glass surface on a similar time scale. Figure 5A shows a typical evolution of the emission signal as a function of time. The abrupt jumps of the signal are characteristic of single-molecule behaviors.

One possible mechanism for the intensity jumps is molecular reorientation on the surface. To test this possibility, we modulated the polarization of the excitation light between the parallel and the perpendicular directions with respect to the molecular transition dipole (parallel to the surface).[19] The fluorescence intensity of another molecule during such a polariza-

(34) Girard, C.; Dereux, A. *Rep. Prog. Phys.* **1996**, *59*, 657.
(35) Novotny, L. Ph.D. Dissertation, Swiss Federal Institute of Technology, ETH No. 11420, 1996.
(36) Yang, W. H.; Schatz; G. C.; Van Duyne, P. *J. Chem. Phys.* **1995**, *103*, 869.
(37) See, for example: Foot, C. S.; Clennan, E. L. In *Active Oxygen in Chemistry*; Foote, C. S., Valentine, J. S., Greenberg, A., Liebman, J. F., Eds.; Blackie Academic & Professional: Glasgow, U.K., 1995; p 105.
(38) Ambrose,W. P.; Goodwin, P. M.; Martin, J. C.; Keller, R. A. *Phys. Rev. Lett.* **1994**, *72*, 160.

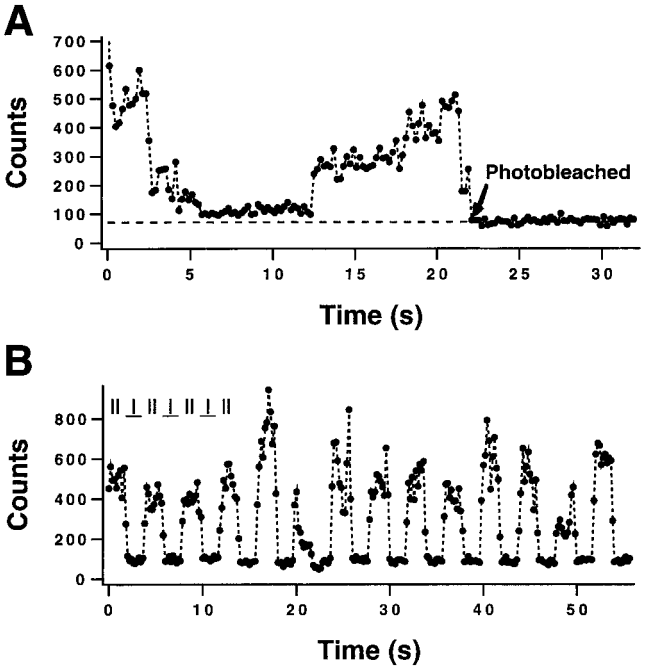

Figure 5. (A) Emission intensity as a function of time (0.2-s bins) for a single sulforhodamine 101 molecule on a glass surface excited with 594-nm light from a NSOM tip. Sudden intensity jumps occur before the signal drops to the background level (dashed line) due to photobleaching. (B) The excitation polarization is modulated (0.25 Hz) between parallel and perpendicular directions of the transition dipole of a different molecule. A constant signal at the background level is observed for the perpendicular excitation while there are sudden fluctuations in the emission signal derived from parallel excitation. This indicates that molecular reorientation is not the cause of the sudden intensity jumps observed in (A) (from ref 19).

tion modulation is shown in Figure 5B. The signal undergoes abrupt jumps with the parallel polarized excitation, but remains at the background level with the perpendicularly polarized excitation. This observation ruled out the possibility of molecular reorientation as the origin of the intensity fluctuations, and we attributed the intensity fluctuations to the variations in the absorption cross section at the excitation wavelength resulting from spectral fluctuations.[19] Although Figure 5B indicates a "stationary" orientational trajectory, this experiment demonstrated the feasibility of recording the orientational trajectory of a chromophore, which will allow direct monitoring of motions during dynamical processes such as protein folding. Until now, such a single-molecule trajectory could only be calculated by molecular dynamics simulations on the femtosecond to nanosecond time scales. Although no noticeable diffusional motion has been observed in this particular system, Schmidt et al. have recently recorded Brownian-motion trajectories of single chromophores in a fluid lipid membrane, which demonstrated the promise for detailed studies of transport properties in biological membranes on the $10^{-2}-10^{3}$-s time scale.[39]

Lu and Xie have recently studied spectral fluctuations using the far-field technique.[40] Figure 6A shows a sequence of emission spectra of a single sulforhodamine 101 molecule on a quartz surface recorded with 170-ms collection times. The sample is covered with a PMMA film to prevent fast photobleaching.

(39) Schmidt, Th.; Schutz, G. J.; Baumgartner, W.; Gruber, H. J.; Schindler, H. *J. Phys. Chem.* **1995**, *99*, 17662.

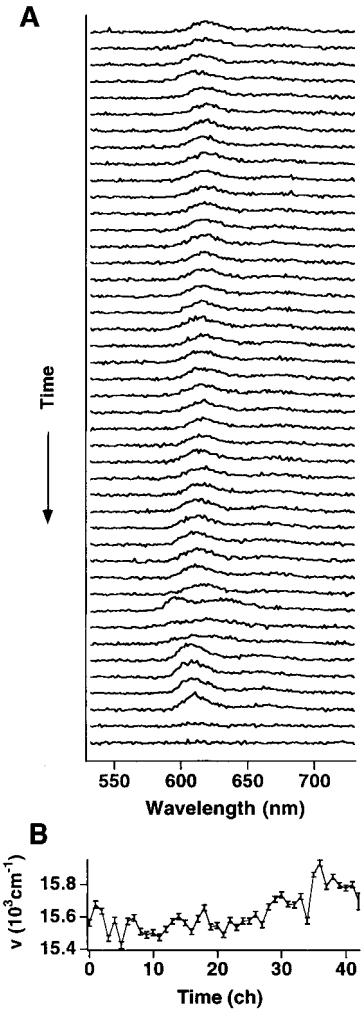

Figure 6. (A) Emission spectra of a single sulforhodamine 101 molecule taken sequentially with 532-nm excitation and 170-ms data collection times before it is finally photobleached. Significant spectral shifts are evident during the course of measurement. The intensity fluctuations (integrated area of each spectrum) are essentially correlated with the spectral fluctuations. (B) Trajectory of the spectral mean (ν) as a function of time (ch, index number of channels). Accepted for publication in *Nature* (ref 40).

Significant spectral fluctuations are evident. The trajectory of the spectral mean is shown in Figure 6B. Fluctuations of total emission intensity (integrated area of each spectrum) indeed arise from and correlate with the spectral fluctuations[40] as we predicted.[19] The spectra in Figure 6A were taken with a low excitation rate (5×10^5 s^{-1}) at which the emission intensity fluctuation is dependent on the excitation wavelength. At high excitation rates, emission intensity is insensitive to spectral fluctuations due to saturation; a different type of intensity fluctuation, however, arises from the fact that molecules are being trapped in the metastable triplet states.[41,42]

To analyze the spectral fluctuations on a statistical basis, we evaluated the autocorrelation function $C(t) = \langle \nu(0)\, \nu(t) \rangle - \langle \nu \rangle^2$ of single-molecule spectral trajectories, ν being the spectral mean in wavenumbers.[40] Figure 7A displays such a $C(t)$, which is a double exponential decay, with the rates for the fast and slow components being $k_1 = 1.85$ s^{-1} and $k_2 = 0.022$ s^{-1},

(40) Lu, H. P.; Xie, X. S. *Nature*, in press.
(41) Bernard, J.; Fleury, L.; Talon, H.; Orrit, M. *J. Chem. Phys.* **1993**, *98*, 850.
(42) Basche, Th.; Kummer, S.; Brauchle, C. *Nature* **1995**, *373*, 132.

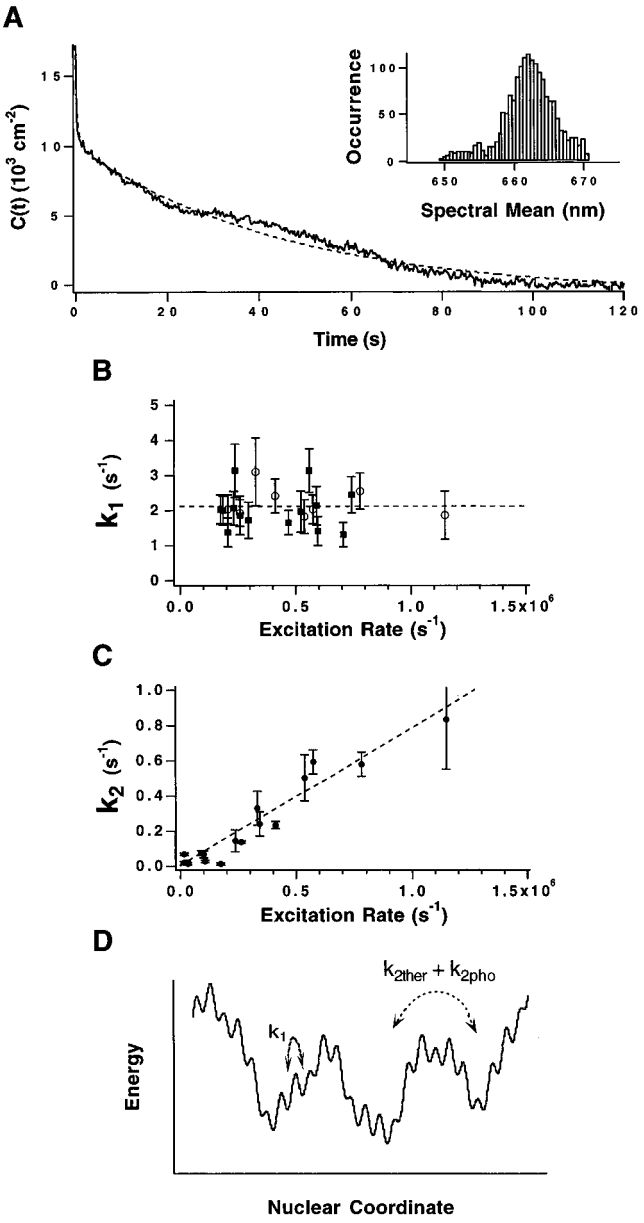

Figure 7. (A) Autocorrelation function of the spectral mean, $C(t) = \langle \nu(0)\nu(t)\rangle - \langle \nu\rangle^2$, of a single sulforhodamine 101 molecule with an excitation rate of 2.6×10^5/s at 594 nm. The dashed line is a fit with a double exponential: $C(t) = \sigma_1^2 \exp(-k_1 t) + \sigma_2^2 \exp(-k_2 t)$, for $t > 0$, with $k_1 = 1.85\ s^{-1}$, $k_2 = 0.022\ s^{-1}$, $\sigma_1^2 = 5000\ cm^{-2}$, and $\sigma_2^2 = 10700\ cm^{-2}$. The inset in (A) shows the distribution of the spectral means accessed by the single molecule in the particular local environment. (B) k_1 as a function of the excitation rate at 594 nm (squares) and at 532 nm (circles). Independent of the excitation rate and wavelength, the fast spectral fluctuation is spontaneous. (C) k_2 as a function of the excitation rate at 532 nm. The linear relationship indicates that the slow spectral fluctuation is photoinduced. A different slope is seen with 594 nm excitation.[40] (D) A schematic of the potential energy surface of the nuclear coordinates. Accepted for publication in *Nature* (ref 40).

respectively. The inset in Figure 7A shows the distribution of the spectral means accessed by the single molecule in the particular local environment. It is important to note that we observed similar spectral fluctuations for every molecule examined within a large population. Molecules in different local environments have spectral mean distributions significantly different in center positions as well as in widths.

Since there is no detectable transitional and rotational diffusion, we attribute the spectral fluctuations to changes of either intramolecular (such as conformational changes of a side chain) or intermolecular nuclear coordinates (such as hydrogen bonds or collective nuclear motions in the interacting environment). The observation that the $C(t)$ of the single molecule is double exponential implies that there exist at least two quasi-independent distributions of spectral means, which are hidden in the distribution in the Figure 7A inset. These two distributions relate to different variations in nuclear coordinates taking place with different rates (k_1 and k_2). In contrast, if the two distributions originated from identical variations in nuclear coordinates, the $C(t)$ would have been a single exponential, with a decay rate being the sum of the two rates. In evaluating many trajectories of many molecules, we observed that (1) the fast component (k_1) is independent of the excitation rate and excitation wavelength (Figure 7B) and (2) the slow component (k_2) is dependent on the excitation rate (Figure 7C) and excitation wavelength.[40]

The fact that k_1 is independent of the excitation rate indicates that the fast component is spontaneous spectral fluctuation (known as spectral diffusion). Although spectral diffusion[43,44] has been studied for single molecules at cryogenic temperatures, the room-temperature spectral diffusion we observed has significantly larger magnitude and involves a thermally activated mechanism. While the broad spectral widths at room temperature (Figure 6A) arise from spectral diffusion on the subpicosecond time scale, the spectral diffusion we observed on the rather long time scale (hundreds of milliseconds) would be extremely difficult, if not impossible, to detect at room temperature in ensemble-averaged experiments.

The linear dependence of k_2 on excitation rate (Figure 7C) clearly indicates that the slow component is photo-induced spectral fluctuation. There are two possible photoinduced mechanisms. First, photoexcitations of a molecule allow access to other potential minima with different spectra through relaxations from the singlet excited state, a phenomenon known as "nonphotochemical hole burning".[45] Single-molecule nonphotochemical hole burning has been observed at cryogenic temperature,[46,47] but with much smaller magnitudes of spectral shifts than observed in our experiment. Second, the photoinduced fluctuations can also be associated with radiationless relaxations, most likely from the triplet state.[40] The energy released in each relaxation event can be dissipated into the substrate through fast vibrational relaxation, and the temperature of the system remains unchanged before the next photoexcitation. However, the energy released can change the nuclear coordinates, and a new spectrum is observed in the subsequent excitations. The slow k_2 is associated with the small quantum efficiency ($\sim 1 \times 10^{-6}$, according to the slope in Figure 7C) for the photoinduced spectral fluctuation due to either mechanism. While more experiments are underway to distinguish between the two mechanisms, we note that the triplet mechanism is inherent to single-molecule experiments due to the inevitable entries to the triplet state ($\sim 1 \times 10^{-3}$ quantum

(43) Ambrose, W. P.; Moerner, W. E. *Nature* **1991**, *349*, 225.
(44) Reilly, P. D.; Skinner, J. L. *J. Chem. Phys.* **1995**, *102*, 1540.
(45) Jankowlak, R.; Small, G. J. *Science* **1987**, *237*, 618.
(46) Orrit, M; Bernard, J. *Phys. Rev. Lett.* **1990**, *65*, 2716.
(47) Moerner, W. E.; Plakhotnik, T.; Irngartinger, T.; Croci, M.; Palm, V.; Wild, U. P. *J. Phys. Chem.* **1994**, *98*, 7382.

efficiency for rhodamine dyes) and the absence of phosphorescence at room temperatures.

Despite the inherent photodriven effects of single-molecule experiments, intrinsic single-molecular dynamics can be studied. For example, within the spectral mean distribution associated with the slow component, both spectral diffusion and photoinduced fluctuation are possible. Being the sum of thermal (k_{2ther}) and photoinduced (k_{2pho}) rates, k_2 is dominated by photoinduced fluctuations under a broad range of excitation rates. Although it is difficult to extrapolate k_{2ther} at zero excitation rate in Figure 7C, k_{2ther} has been determined to be 0.02 ± 0.01 s^{-1} by a scheme in which the excitation light is periodically blocked for a period of "dark time" after each spectrum collection, waiting for spectral diffusion to occur.[40]

The analyses of single-molecule spectral trajectories allowed us to derive properties of the ground state potential energy surfaces in particular environments.[40] The 2 orders of magnitude difference between k_1 and k_{2ther} indicates two distinctly different types of barrier heights in the potential energy surface of the nuclear coordinates. As shown in a one-dimensional cross section of the surface (Figure 7D), the potential minima connected with the small barriers can be easily accessed through thermally activated fluctuation (k_1), whereas the gross potential minima connected with the large barriers can only be accessed through photoexcitation (k_{2pho}) and much slower thermally activated fluctuation (k_{2ther}). The temperature dependence of the thermal fluctuations is being determined in order to obtain the barrier heights. Similar properties of potential energy surfaces have been put forward for proteins.[48] The spectral trajectory analyses of a specific active site in a protein will allow detailed investigation of conformational dynamics and energy landscapes, and their influence to enzymatic reactions.

On a single-molecule basis, a stochastic action of a chemical reaction takes place on the subpicosecond time scale. The rate of a chemical reaction, however, is usually much slower due to the low probability for successful barrier crossing through thermal activation. Single-molecule events of chemical reactions have been directly monitored.[49,50] Single-enzyme activities and their heterogeneity have also been observed.[51,52] Studying single-molecule chemical kinetics in real time, however, requires statistical analyses. On the $10^{-2}-10^{3}$-s time scale, the rate of a reversible chemical reaction on a single molecule can be measured by intensity autocorrelation functions, if the complication of intensity fluctuations due to spectral fluctuations can be minimized. A similar measurement was elegantly demonstrated in the 1970s by Magde, Elson, and Webb[53] on a reacting system composed of a small number of molecules in dynamical equilibrium. Moreover, Wang and Wolynes pointed out that higher order intensity correlation functions of single molecules can yield unique dynamical information,[54] such as non-Poisson statistics and "intermittency"[55] in complex reaction systems, which is not obtainable from ensemble-averaged experiments.

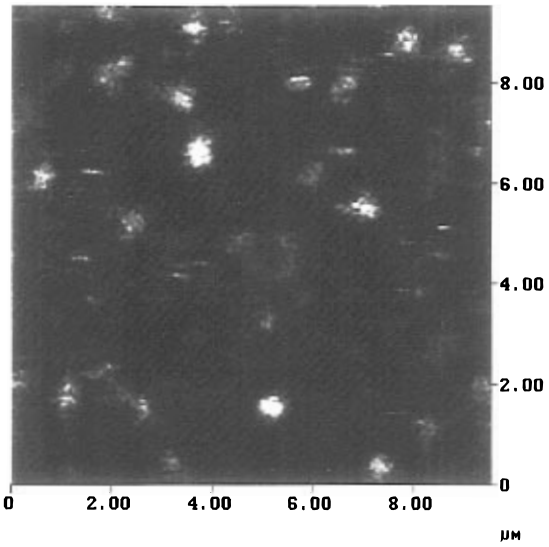

Figure 8. A far-field fluorescence image of single proteins of pentachlorophenol 4-monooxygenase, a 60-kDa enzyme, demobilized in a thin film of agarose gel of 98% water content. Each protein contains a cofactor, flavin adenine dinucleotide (FAD), which is naturally fluorescent in its oxidized form. The FAD fluorescence was excited with 488-nm light.

To indicate the promise of monitoring enzymatic reactions in real time, Figure 8 shows our far-field fluorescence image of single flavoproteins demobilized in an agarose gel of 98% water. The protein pentachlorophenol 4-monooxygenase is a 60 kDa enzyme converting pentachlorophenol to tetrachloro-*p*-hydroquinone.[56] The active site of the enzyme is flavin adenine dinucleotide (FAD), which is naturally fluorescent in its oxidized form. Each spot in Figure 8 corresponds to a single enzyme with a single fluorescent FAD. Fluorescence and topographic images of single photosynthetic antenna proteins, each containing six natural fluorophores, have also been obtained with near-field microscopy.[7,57]

Probing Single-Molecule Dynamics on the Picosecond to Nanosecond Time Scale

The repetitive excitations ($<10^7$/s) in single-molecule experiments do not permit monitoring single-molecule trajectories in real time on the picosecond and nanosecond time scale. For a repeatable photoinduced process, however, measurements of single-molecule fluorescence lifetimes using ultrashort pulse trains allow determination of the temporal survival probability on this time scale. In addition to the radiative and nonradiative processes discussed earlier, other photoinduced dynamical processes, for example, the energy transfer between a single donor acceptor pair,[58] can be studied. It is particularly interesting to measure the single-molecule chemcial kinetics of photoinduced reactions, such as photoinduced electron transfer. Conventional measurements done on large ensembles of molecules often exhibit multiexponential

(48) Frauenfelder, H.; Wolynes, P. G. *Phys. Today* **1994**, *47*. 58.
(49) Collinson, M. M.; Wightman, R. M. *Science* **1995**, *268*, 1883.
(50) Funatsu, T.; Harada, Y.; Tokunaga, M.; Saito, K.; Yanagida, T. *Nature* **1995,** *374*, 555.
(51) Xue, Q. F.; Yeung, E. S. *Nature* **1995**, *373*, 681.
(52) Craig, D. B.; Arriaga, E. A.; Wong, J. C. Y.; Liu, H.; Dovichi, N. J. *J. Am. Chem. Soc.* **1996**, *118*, 5245.
(53) Magde, D.; Elson, E.; Webb, W. W. *Phys. Rev. Lett.* **1972**, *29*, 705.
(54) Wang, J.; Wolynes, P. *Phys. Rev. Lett.* **1995**, *74*, 4317.
(55) Zeldovich, Y. B.; Ruzmaikin, A. A.; Sokoloff, D. D. *The Almighty Chance*; World Scientific: River Edge, NJ, 1990.
(56) Xun, L.; Topp, E.; Orser, C. S. *J. Bacteriol.* **1992**, *174*, 5745.
(57) Dunn, R. C.; Allen, E. V.; Joyce, S. A.; Anderson, G. A.; Xie, X. S. *Ultramicroscopy* **1995**, *57*, 113.
(58) Ha, T.; Enderle, Th.; Ogletree, D. F.; Chemla, D. S.; Selvin, P.; Weiss, S. *Proc. Nat'l Acad. Sci. U.S.A.* **1996**, *93*, 624.

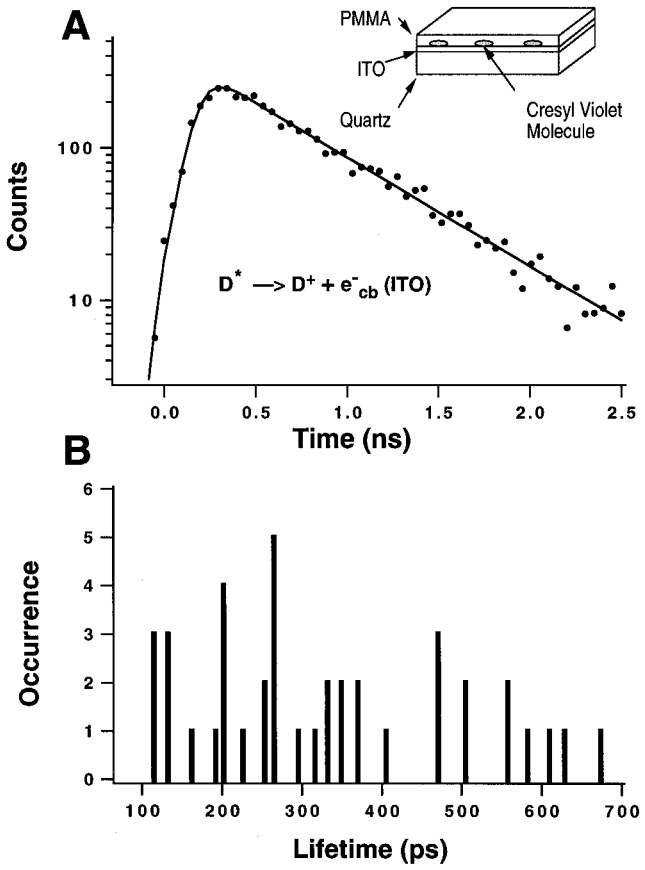

Figure 9. (A) Fluorescence decay of a single cresyl violet molecule dispersed on an ITO film. The fast decay is due to interfacial electron transfer from the excited molecule (D*) to the conduction band of ITO. The solid line is a single-exponential fit (480 ps, $\chi^2 = 1.14$) convoluted with the instrumental response function (FWHM 160 ps). (B) Histogram of emission lifetimes for 40 different molecules examined, revealing a broad distribution of site-specific electron transfer kinetics. Submitted for publication in *J. Phys. Chem.* (ref 59).

kinetics which can arise from different origins and represent a major obstacle in understanding detailed mechanisms of chemical reactions. The single-molecule chemical kinetics, on the other hand, can provide more detailed information. For example, the electron transfer of a single photosynthetic unit can be studied in the native membrane environment free from the complications of sample heterogeneity.

Lu and Xie recently demonstrated the measurement of single-molecule chemical kinetics for the interfacial electron transfer from cresyl violet molecules to an indium−tin oxide (ITO) substrate.[59] The interest in photoelectrochemistry has resulted in extensive work on dye sensitization at semiconductor surfaces. The subject has been critically reviewed.[60,61] It has been well established that, upon photoexcitation, interfacial electron transfer occurs from the excited dye molecule to the conduction band of the semiconductor substrate, the rate of which can be measured by the fluorescence decay of the dye molecule. Many experiments on similar systems showed multiexponential kinetics, the origin of which was not well understood.

Figure 9A shows the fluorescence decay of a single cresyl violet molecule, which is single exponential with a time constant of 480 ps. The fast decay is dominated by electron transfer kinetics and is not influenced by radiative rates. Interestingly, we found a wide distribution of lifetimes (Figure 9B) for the molecules examined. On the basis of Figure 9B, measurements made on large ensembles of molecules would have more than 20 exponentials, which is impossible to resolve in practice. Our single-molecule results indicate that the origin of the multiexponential behavior of this system arises from the heterogeneity of the "static" sites.[59]

We have not observed multiexponential kinetics of single molecules in this system, nor have we observed any noticeable changes of lifetimes during the measurements. However, we note that multiexponential kinetics for a single molecule would be possible if slow variations of nuclear coordinates (spectral diffusion) result in changes of the rate during the course of the measurement. This is especially possible for glassy or polymeric systems such as proteins in which slow relaxation processes exist. With complications from site heterogeneity avoided, it is now feasible to probe dispersed kinetics, i.e, the stretched exponential behavior often present in these systems.

Conclusion

In this Account, I have given a brief survey of recent activities in studying single-molecule behaviors in ambient environments. The electromagnetic interactions of a single molecule with a nanostructure with arbitrary geometry can now be probed and computed with great detail. Single-molecule dynamics can be studied on two vastly different time scales. On the $10^{-2}-10^{3}$-s time scale, single-molecule spectral trajectories provide information regarding the energy landscape and dynamics of a fluorophore in a particular local environment. On the picosecond to nanosecond time scale, site-specific chemical kinetics of single molecules can be measured. Initial studies have already provided unique and detailed information not accessible from ensemble-averaged experiments. Room-temperature single-molecule spectroscopy with near-field and far-field microscopy has emerged from the development stage to the application stage. Single-molecule studies will not only create new opportunities across a broad range of disciplines, but also enable researchers to obtain new information on molecular interactions and chemical dynamics in complex systems in many years to come.

I gratefully acknowledge the efforts of a group of talented individuals responsible for the studies summarized herein: Robert Dunn, Peter Lu, Randy Bian, Vey Allen, Erik Sanchez, and Gary Holtom. It is also a pleasure to acknowledge Professor Peter Leung at Portland State University, Professor Laurens Mets at the University of Chicago, and Professor Luying Xun at Washington State University for fruitful collaborations. I am indebted to Dr. Steve Colson and colleagues for creating the stimulating environment at the Environmental Molecular Sciences Laboratory. The research was supported by the U.S. Department of Energy's (DOE) Basic Energy Sciences, Chemical Sciences Division, with instrument development support from DOE's Energy Research Laboratory Technology Application program and Digital Instruments, Inc.

AR950246M

(59) Lu, H. P.; Xie, X. S. Submitted to *J. Phys. Chem.*
(60) Hagfeldt, A.; Gratzel, M. *Chem. Rev.* **1995**, *95*, 49.
(61) Willig, F. In *Surface Electron Transfer Processes*; Miller, R. J. D., McLendon, G. L., Nozik, A. J., Schmickler, W., Willig, F., Eds.; VCH Publishers: New York, 1995; p 167.